EXPERIMENTS AND NUMERICAL PREDICTIONS OF FLOW RATES AND AERO-ACOUSTICS FROM SMALL RADIAL NOTEBOOK BLOWERS

Jessica GULLBRAND, Willem M BELTMAN

Intel Corporation, 2111 NE 25th Avenue, 97124 Hillsboro, Oregon, USA

SUMMARY

The notebook performance depends upon the cooling capability of the blower. Optimized airflow and reduced noise are necessary to maximize system performance within ergonomic limits. In this investigation, the performance of a notebook blower is investigated numerically and compared with experimental data. The acoustic noise generated by the blower is predicted, when the blower is mounted in free field or in a bracket, which is done during experimental evaluation. Good repeatability is shown in the measurements of the blade-pass-frequency (BPF). The noise level at the BPF is the highest peak value and the predictions show promise, but that accurate aero-acoustic predictions are still challenging.

INTRODUCTION

The performance of a notebook system depends upon the thermal cooling capacity of the blower/heat exchanger combination, which in turn is dictated by the effective airflow rate produced by the blower. The cooling capacity increases with increased airflow, but so does the acoustic noise. However, ergonomic limits of the acoustic noise from notebooks need to be adhered to, which causes most notebook blowers to operate below maximum rotational speeds. This leads to a scenario in which the performance of many notebook systems is acoustically limited. It is therefore of great importance to optimize notebook blower designs for maximum flow rate and low acoustic noise. This optimization has historically been performed by building expensive prototypes and performing experimental investigations.

Accurate numerical techniques are required to numerically optimize the blower designs to reduce design time and prototype cost. It is only recently that numerical characterization of airflow and acoustic performance has received increased attention [1-6], due to the availability of advanced simulation techniques in commercial software. Previous investigations of radial blowers using computational fluid dynamics (CFD) have shown that the airflow performance can be accurately predicted [1-4]. The aero-acoustic predictions are still challenging for this type of flow [3-4]. However, aero-acoustic capabilities are becoming more accessible, since several commercial software programs now have the capability of generating three-dimensional flow fields and using that as input data for the aero-acoustic predictions [7]. The accuracy of these acoustic models to predict noise generated by small radial blowers need to be determined.

In this paper, numerical simulations of a typical radial notebook blower are performed to first determine accuracy of the airflow and pressure performance of the blower when compared to experimental data. The flow field simulations are performed using unsteady Reynolds-Averaged Navier-Stokes (URANS) equations. Thereafter, aero-acoustic simulations are undertaken. Two different blower setups are investigated: one setup where the blower is in free field and the other one where the blower is mounted in a bracket. The bracket is generally used in experimental evaluation of notebook blowers, when the acoustic performance as a function of back pressure is determined in an acoustic plenum [1]. Here, the impact of the bracket on the acoustic response is measured and compared to predictions. The Ffowcs-Williams and Hawkings (FWH) analogy [8] is used in the aero-acoustic predictions.

EXPERIMENTS

The notebook blower investigated in this study is shown in Figure 1. The outer dimensions of the blower are 60x53x10 mm. The blower has an integrated DC brushless motor operating nominally at 5 V. The blower has two inlets: one primary inlet on the top and one secondary inlet on the bottom. The secondary inlet area is slightly smaller than the primary one, since three motor struts are blocking part of this inlet. The blower has a single outlet. A blower with these dimensions is typically used in a medium-sized or thin form factor notebook.

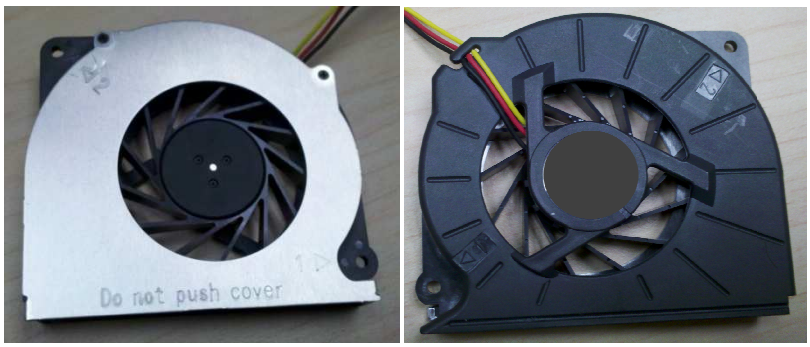

Figure 1: Small radial notebook blower

Flow and Pressure Performance

The flow measurements presented herein were performed on an airflow chamber (AFC) manufactured by Hill Engineering, model 798. The chamber consists of a plenum to which the blower is connected, and a second integrated blower to apply the desired back pressure to the plenum. The total flow of the blower being tested is measured with a laminar flow element. This system conforms to ANSI/ASHRAE 51 [9], and can determine both the volumetric flow with an uncertainty of < 1 % ACFM reading, and the static pressure with an uncertainty of +/- 0.006 inW.C..

Acoustic Performance

The acoustic measurements were performed in an ISO 3744 [10] compliant hemi-anechoic chamber. The sound pressure measurements inside the anechoic chamber were conducted with four Bruel & Kjaer (B&K) 4189 microphones that were calibrated with a B&K 4231 sound calibrator. The microphone locations are 0.25 m in front of the primary inlet (front), 0.25 m behind the secondary inlet (back), and 0.25 m on each side of the blower (left and right) as shown in Figure 2. The acoustic noise generated for the two configurations, blower in free field and blower with bracket, were measured. The bracket is made of ABS material, and the outer dimensions are 90x45x5.25 mm. The opening for the blower outlet is centered in the bracket. The bracket is shown

in Figure 2 (right). Results from the front and the left microphone locations will be presented in this investigation. Three different blowers of the same model were measured and three measurements were performed for each blower operating at 4500 RPM. A 1 Hz resolution is used for the Fast Fourier Transformation (FFT) to determine Sound Pressure Level (SPL) as a function of frequency for the measured values.

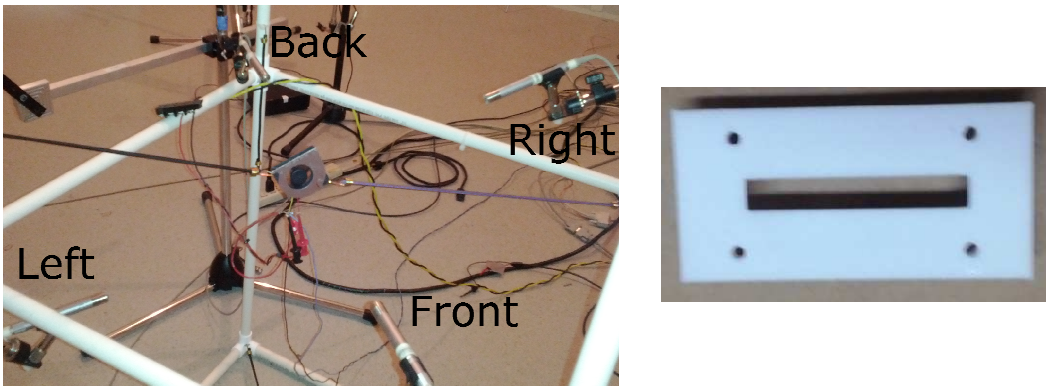

Figure 2: Blower suspended in free field (left) and blower bracket (right)

NUMERICAL SIMULATIONS

Flow and Pressure Simulations

The flow and pressure performance was modeled using three-dimensional unsteady Reynolds-Averaged Navier-Stokes (URANS) equations. The averaging procedure introduces a term that cannot be resolved, and therefore it has to be modeled. A two transport equation model is used in the simulations presented here: the shear-stress transport (SST) k-ω model. One transport equation is solved for the turbulent kinetic energy, k, and one for the specific dissipation rate, ω. Additional details regarding the models can be found in the Fluent® manual [8].

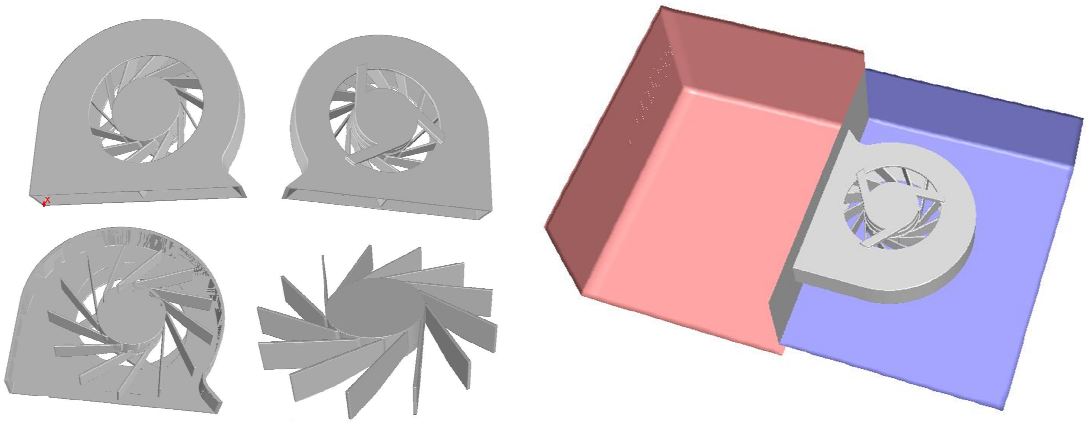

Figure 3: Blower geometry and computational domain around the blower consisting of blue inlet domain and red outlet domain

The full blower geometry is modeled in the simulations. The numerical geometries are shown in Figure 3. The footprint of the blower is 60x53 mm, and the thickness of the casing is 10 mm. The motor struts on the secondary inlet add an additional 1 mm to the blower thickness. The diameter of

the rotor is 48 mm, and the blade height at the tip is 7 mm. The computational domain consists of a rectangular inlet volume around the blower and a rectangular outlet volume. The inlet domain is 100 mm wide and 80 mm long with a height of 32.5 mm. The outlet domain has the same length and width as the inlet domain, but it is 52.5 mm in height. The blower is centered in the inlet domain (width and height wise) with the outlet of the blower placed on the boundary between the inlet and outlet domains. The surface between the two domains is either simulated as a wall for the bracket model or as an interior surface for the free field blower model. It should be noted that the bracket dimensions (90x45 mm) are smaller than the surface (100x52.5 mm) used in the simulations to model the bracket.

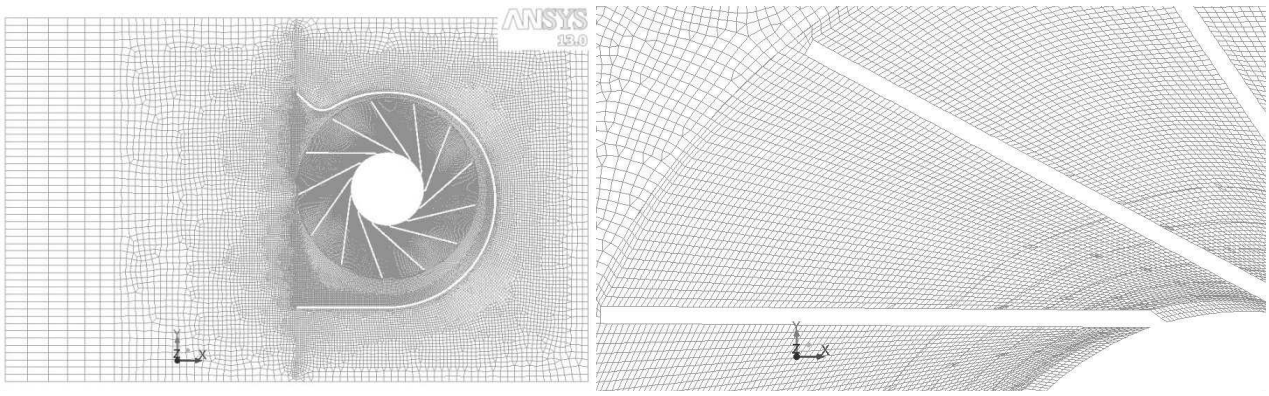

Figure 4: Numerical mesh used in simulations

The numerical mesh used in this investigation applies a sliding mesh interface between the rotor domain and the stationary domain. This numerical interface is conformal, and there are 33 cells for each blade pass as seen in Figure 4. The rotational speed is fixed in the simulations to 4500 RPM, and the time step is 31.08 μs. The total mesh size is nominally 6 million cells. An unconstrained pressure-inlet condition is used together with a pressure-outlet condition for the inlet and outlet domains respectively. The pressure is increased in the outlet domain to predict the flow rate as a function of back pressure (i.e. fan curve). The flow is assumed to be incompressible, and double precision is used in all simulations.

Acoustic Simulations

The aero-acoustic approach applies the unsteady flow field results as an input data to the Ffowcs-Williams and Hawkings (FWH) model directly in Fluent [8]. The complete solution consists of surface and volume integrals. The surface integrals represent the noise sources of a monopole and dipole character, and include some quadrupole character. The volume integrals represent the quadrupole sources. In the current simulations, the volume integrals are neglected. The dropped volume integrals result in an absence of broadB(A)nd acoustic sound. However, the effect of the dropped volume integrals is expected to be minor, since tonal noise dominates the noise emissions. In this investigation, only the tonal noise is predicted and compared to experimental results. Acoustic data is gathered in the simulations for more than 15 full rotations of the rotor. It should be noted that the FWH model was developed for radiation of acoustic sound in free field conditions and the current geometry with the rotor in a blower casing violates this assumption. However, the blower can be considered a compact noise source up to 6 kHz, and therefore the comparison between experiments and simulations is performed up to the 6 kHz limit.

RESULTS

Flow Field

The airflow through the blower is shown in Figure 5. It can be seen that the outlet of the blower is relatively short and wide, which results in several distinct jets exiting the blower outlet. The largest jet is generated by the increased gap distance between the rotor tip and the casing on the opposite side of the cut-water location. The jet leaving the outlet close to the cut-water is exiting at the same angle as the casing. The velocity distribution at the blower outlet needs to be taken into account for a given blower when designing the heat exchanger for optimal cooling capacity. An enlarged vector plot of the cut-water region shows a small recirculation zone generated close to the cut-water location.

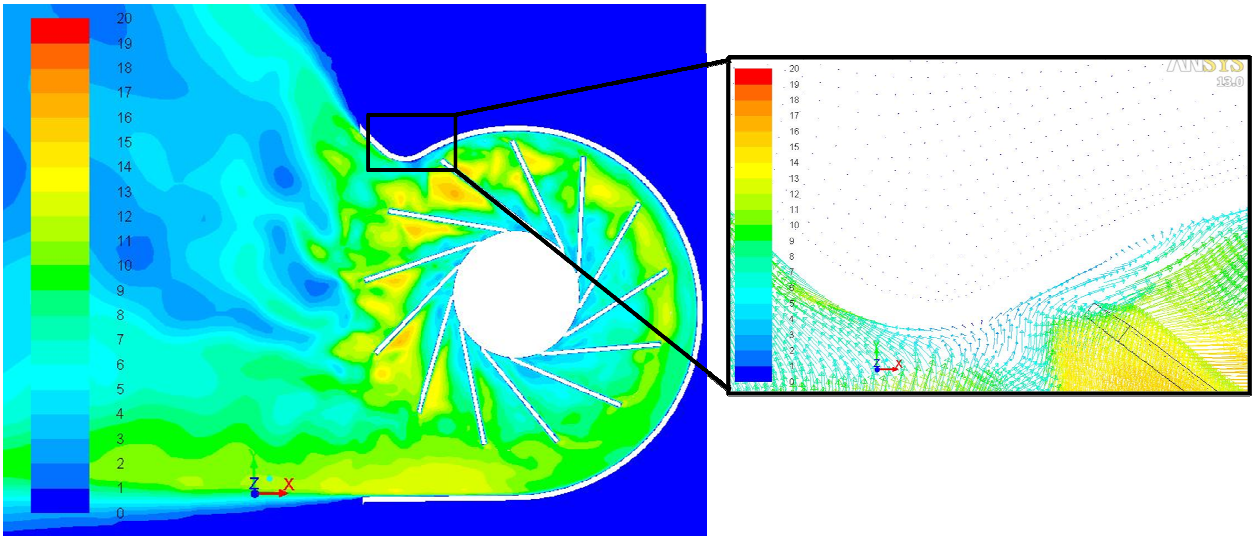

Figure 5: Instantaneous velocity magnitude in m/s through the mid-plane of the blower at 4500 RPM

Flow and Pressure Performance

The blower performance is shown as a fan curve in Figure 6, when the blower is operating at a rotational speed of 4500 RPM. The rotational speed was fixed in both experiments and simulations. In the experiments, the rotational speed changes slightly with ± 10 RPM throughout the measurement. Good agreement between the measurements and predictions is shown in the Figure. The discrepancy is the largest at 50 Pa, where it is 10 %. The results are similar to what has previously been reported for another radial notebook blower [1-4].

The inlet and outlet domains of the blower are separated with a wall in both the simulations and the experiments for the fan curve presented in Figure 6. Simulations showed that at free flow conditions (0 Pa back pressure) and free field conditions (no wall separation between inlet and outlet domains), the flow rate through the blower did not change. However, a removal of the separating wall allows surrounding air to be entrained into the jet exiting the blower outlet. This results in an increase of airflow with 27 % through the entire computational

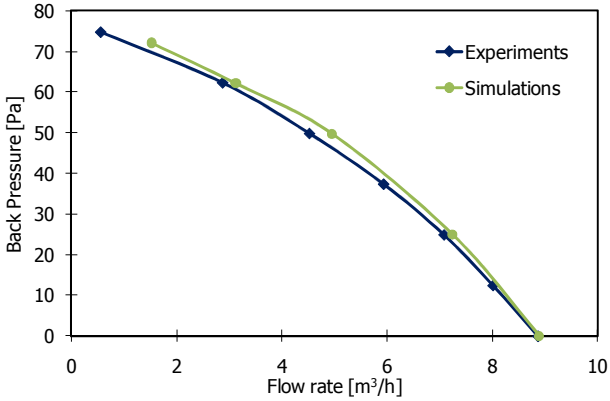

Figure 6: Fan curve for blower in bracket condition at 4500 RPM

domain. The airflow generated between the inlet and the outlet domain due to the entrainment is shown in Figure 7 for the free field condition and the bracket case (no airflow).

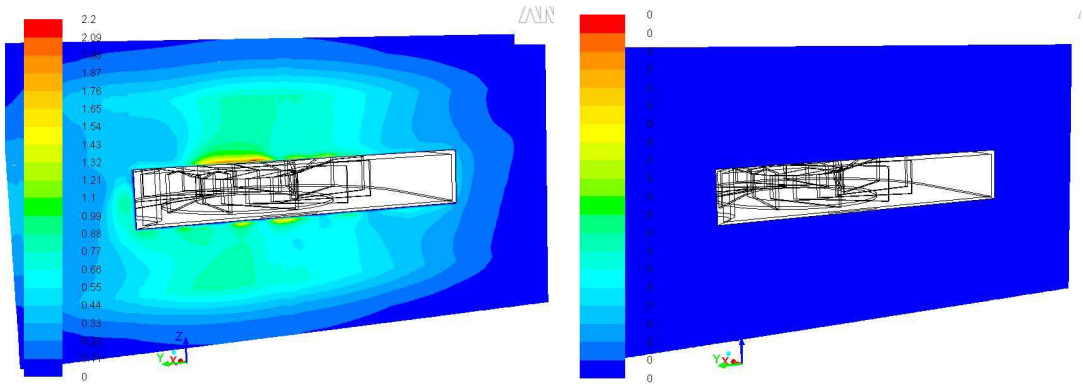

Figure 7: Instantaneous velocity magnitude in m/s from inlet to outlet region for the free field condition (left) and bracket (right)

Acoustic Performance – Free Field

The acoustic response measured in front of the primary/unconfined inlet for three different blowers of the same model is shown in Figure 8. Significant differences between the blowers can be observed. A detailed statistical analysis of the peak sound pressure level at the blade-pass-frequency (BPF) and its harmonics shows that the variations in peak levels are a strong function of the harmonic. The statistical range needs to be considered for each harmonic peak value when comparing the simulation results with the experimental data. The averaged peak value for the BPF (975 Hz) is 27 dB(A), and it is the highest peak in the spectrum. The peak value of the second harmonic is 17 dB(A). The experiments show peaks at low frequencies below the blade-pass-frequency (BPF), which is likely due to motor noise (75 Hz harmonics). The range from the 25 % to 75 % quartile is 2 dB(A) for the first harmonic (BPF), and the second harmonic has a range of 6 dB(A) in the front measurement location.

The averaged acoustic response measured in the left microphone location is shown in Figure 9. The peak value at the BPF is 36 dB(A), which is significantly higher than for the front location. The second harmonic is 19 dB(A). The range from the 25 % to 75 % quartile is 1 dB(A) for the first harmonic (BPF), and the second harmonic shows a very large spread of 12 dB(A).

The aero-acoustic prediction results using the FWH approach are compared to the experimental data for the BPF and higher harmonics. The 25 %, 50 % (median), and 75 % quartile from the sound pressure measurements are shown together with the simulated data for the first six harmonics in Figure 10. It is the first BPF that generates the highest peak value for this blower, and it is this peak that needs to be reduced first when optimizing the blower performance. It is therefore essential to accurately predict the tonal component at the BPF. The results show that the first harmonic is over-predicted in both measurement locations with 6 dB(A) for the left location and 9 dB(A) for the front. This over-prediction can be a result of the increased airflow in the computational domain, which is caused by entrainment of surrounding air in the blower outlet flow (shown in Figure 7).

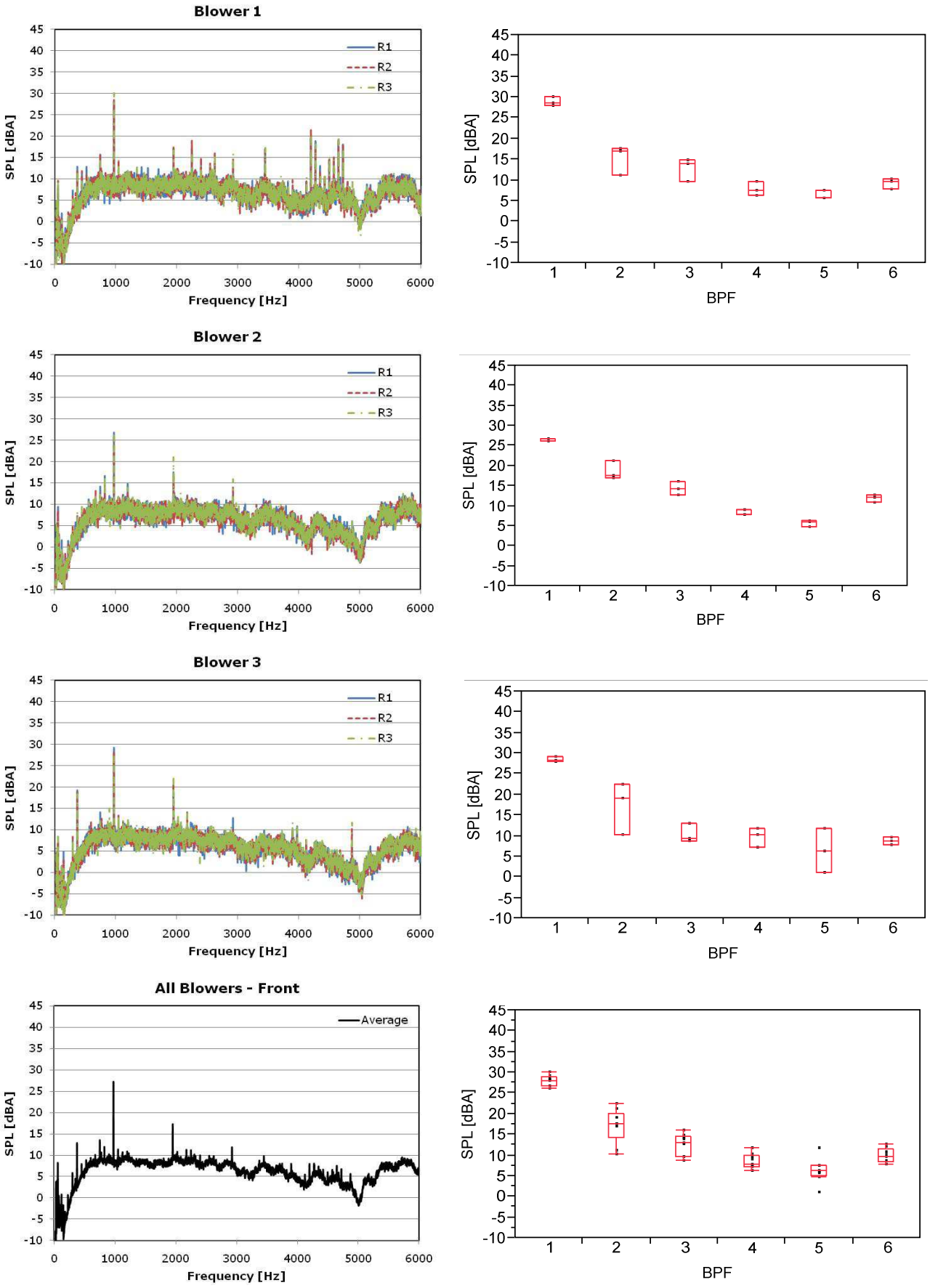

Figure 8: Acoustic experimental data (front position) for three different blowers (same model) in free field condition and statistical analysis of BPF harmonics showing 25 % and 75 % quartile values by the red boxes

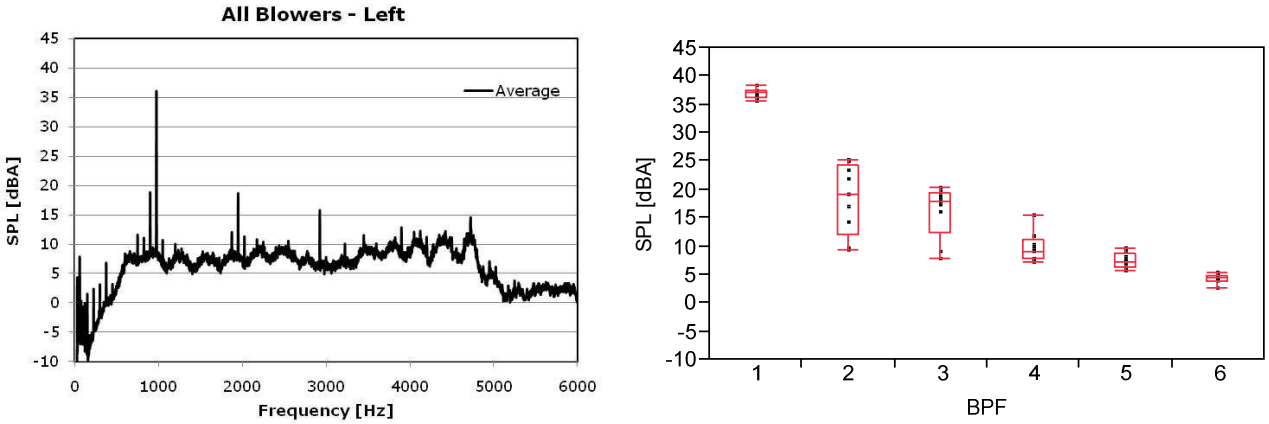

Figure 9: Acoustic experimental data (left position) averaged over three different blowers in free field condition and statistical analysis of BPF harmonics showing 25 % and 75 % quartile values by the red boxes

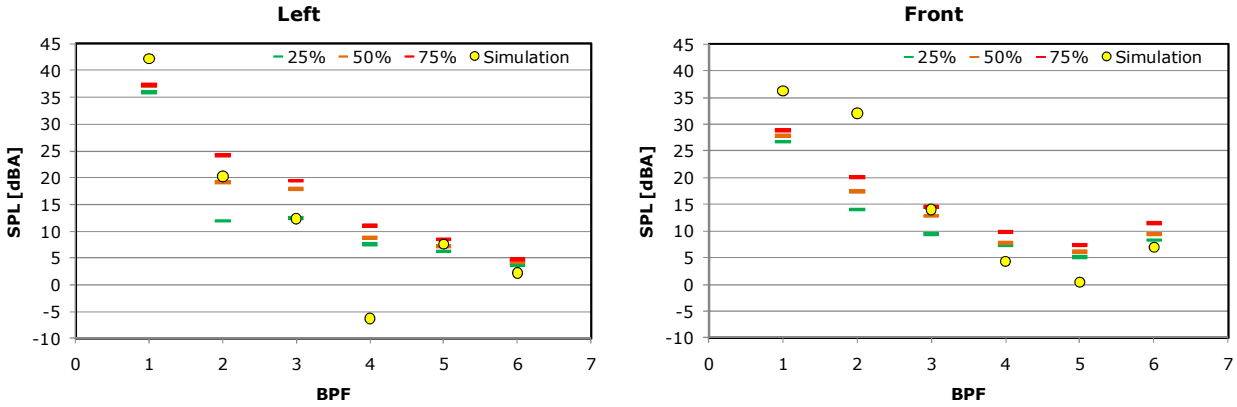

Figure 10: Sound pressure level as a function of BPF harmonics for measurements (25 %, 50 % and 75 % quartile) and simulations for left and front measurement locations

Acoustic Performance – Bracket

The acoustic noise emission from the three different blowers, when mounted on the bracket is shown in Figure 11. The figure shows that there are variations between blowers, between experiments for a single blower, and that there are differences compared to the free field setup. A detailed analysis of the peak sound pressure levels at the blade-pass-frequencies shows some interesting effects. First, the bracket results in a sharp increase in the variations between the blowers. The mounting introduces a significant source of variability in the results. For the front measurement location, the sound pressure level at the BPF increases slightly from the free field case. The averaged peak value for the BPF (975 Hz) is 30 dB(A), and it is the highest peak in the spectrum. The peak value of the second harmonic is 24 dB(A). The range from the 25% to 75% percentiles is 4 dB(A) for the first harmonic and 18 dB(A) for the second harmonic. The results clearly show very large variations of the second harmonic when mounted on the bracket.

The averaged acoustic response measured in the left microphone location is shown in Figure 12. The peak value at the BPF is 36 dB(A), which is unchanged compared to the free field experiments. The second harmonic is 11 dB(A), which is lower than in the free field. The range from the 25 % to 75 % quartile is 2 dB(A) for the first harmonic (BPF), and the second harmonic has a spread of 4 dB(A).

The sound pressure levels at the BPF and its higher harmonics both measured and predicted are compared in Figure 13, when the blower is mounted in the bracket. The 25 %, 50 % (median), and 75 % quartile from the sound pressure measurements are shown together with the simulated data for the first six harmonics in the Figure. The results show that the first harmonic is accurately predicted

for the left measurement location, while the simulations significantly under-predict the BPF with 17 dB(A) for the front location. The amount of under-prediction for the front location is larger than previously observed [1-4] and additional analysis is necessary to better understand the underlying cause.

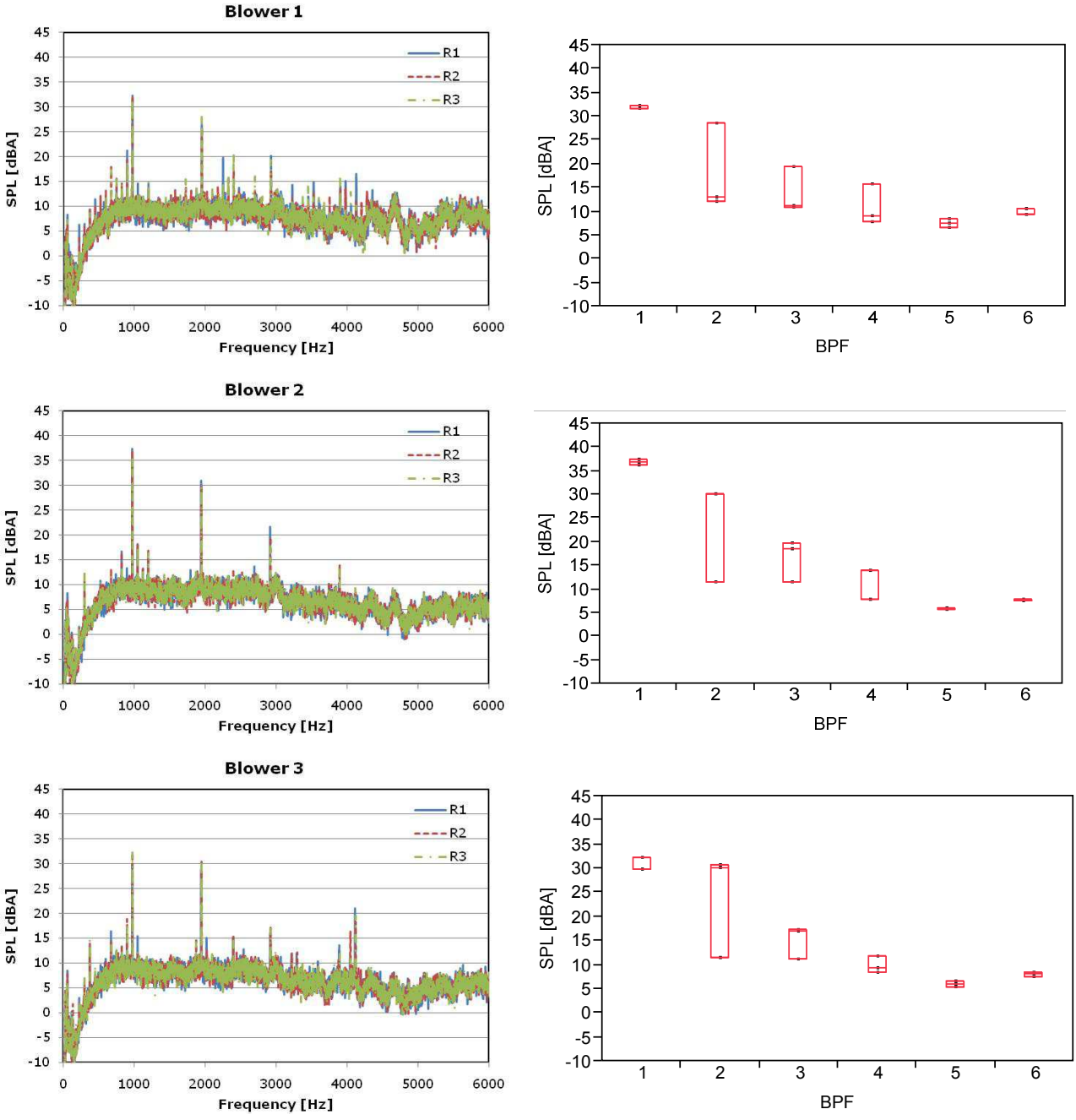

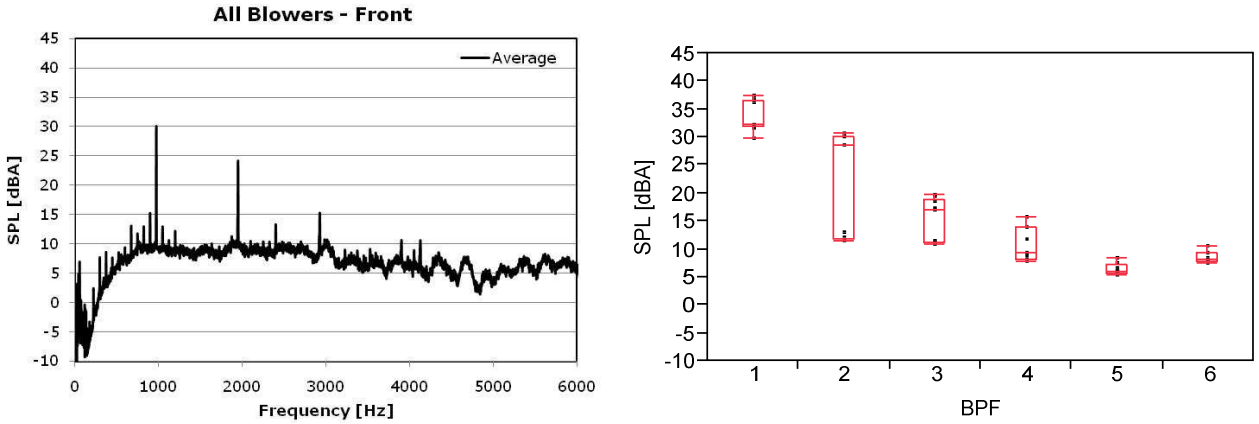

Figure 11: Acoustic experimental data (front position) for three different blowers (same model) in bracket condition and statistical analysis of BPF harmonics showing 25 % and 75 % quartile values by the red boxes

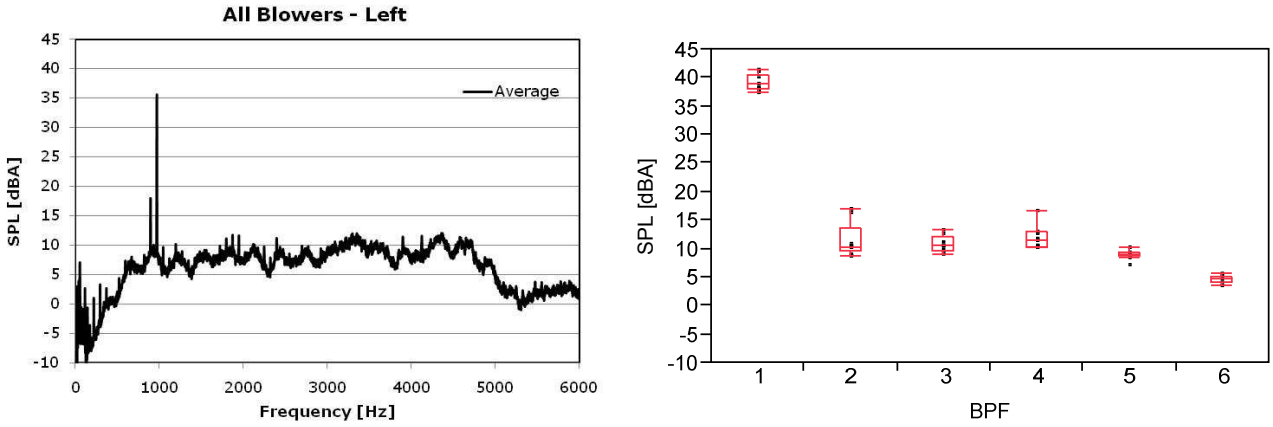

Figure 12: Acoustic experimental data (left position) for three different blowers in bracket condition and statistical analysis of BPF harmonics showing 25 % and 75 % quartile values by the red boxes

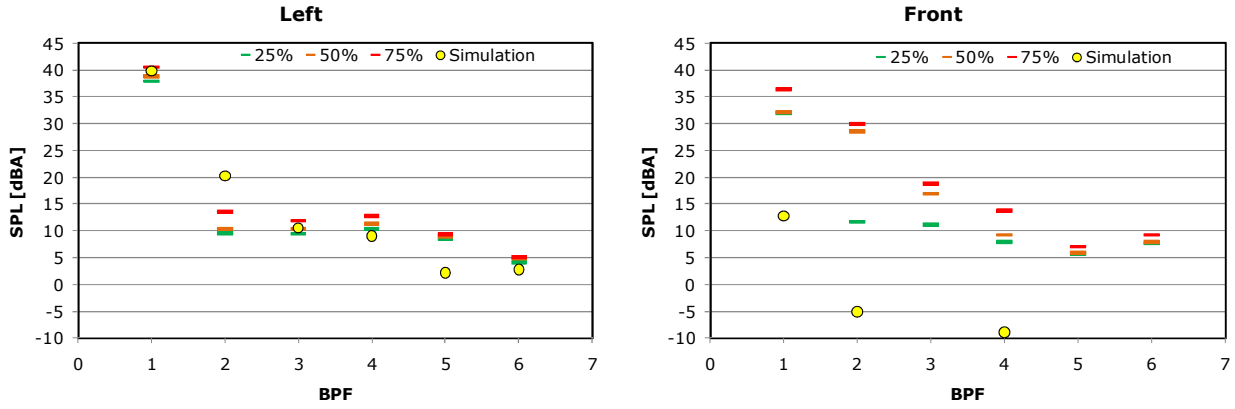

Figure 13: Sound pressure level as a function of BPF harmonics for measurements (25 %, 50 % and 75 % quartile) and simulations for left and front measurement locations

Acoustic Performance – Bracket versus Free Field

A direct comparison of the sound pressure levels from the blower when mounted on a bracket versus in free field condition is given in Figure 14. The results show that the variability increases when the blower is mounted on the bracket, especially for the second harmonic. For the front measurement location, the peak value for the first blade-pass-frequency shows an increase that is significant, whereas for the left measurement location it decreases slightly.

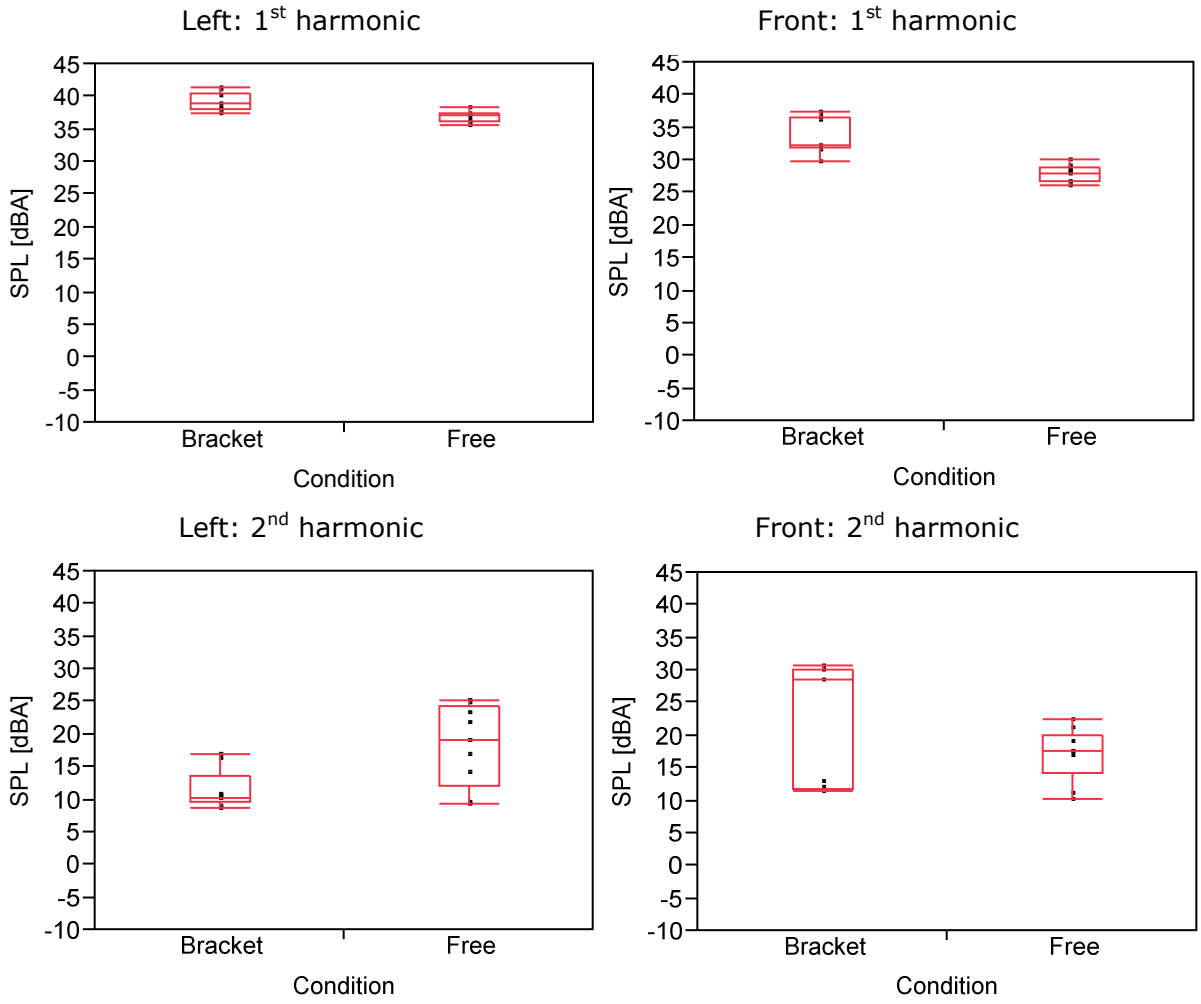

Figure 14: Comparison of sound pressure levels for the blower mounted in a bracket and in free field condition at left and front measurement locations

CONCLUSIONS

The performance of a small radial notebook blower was investigated through detailed unsteady three-dimensional numerical simulations and experimental measurements. Good agreement was observed for airflow and pressure performance between measurements and numerical predictions. The flow fields were then used to predict the aero-acoustic noise generated by the blower. The Ffowcs-Williams and Hawkings (FWH) analogy was used for the aero-acoustic predictions. Two different blower setups were analyzed: one in free field, and the other one mounted in a bracket. Good measurement repeatability was shown at the blade-pass-frequency, while large variability was shown for the second harmonic. The acoustic predictions show promise for capturing the first harmonic. However, accurate aero-acoustic predictions are still challenging and further research is needed to separate out effects from different sources in the blower.

BIBLIOGRAPHY

[1] M.A. MacDonald, J. Gullbrand, Y. Nishi and E. Baugh, "*Notebook blower inlet flow and acoustics: Experiments and simulations*", Noise Control Eng. J., 57(3/4), July/Aug special edition on fan noise, **2009**

[2] J. Gullbrand, W.M. Beltman and M.A. MacDonald, "*Investigation of fan law accuracy for small scale electronic cooling blowers*", Proceedings in Inter-Noise 2009 August 23-26, **2009**

[3] J. Gullbrand and W.M. Beltman, "*Aero-acoustic simulations of small scale electronic cooling blowers*", Proceedings in NoiseCon 2010 April 19-21, **2010**

[4] J. Gullbrand and W.M. Beltman, "*Aero-acoustic simulations of small radial blowers*", Proceedings in NoiseCon 2011, July 25-27, **2011**

[5] Q. Liu, D. Qi and Y. Mao, "*Numerical calculation of centrifugal fan noise*", Proceedings IMechE, 220, Part C, 1167 – 1177, **2006**

[6] R. Ballesteros-Tajadura, S. Velarde-Suarez and J.P. Hurtado-Cruz, "*Noise Prediction of a centrifugal fan: Numerical results and experimental validation*", Journal of Fluid Eng., 130, **2008**

[7] J. Defoe and C. Novak, "*Review of computational aeroacoustics for application in electronics cooler noise*", Canadian Acoustics, 34(3), 76-77, **2006**

[8] Fluent® manual, http://www.fluentusers.com/fluent/

[9] ANSI/ASHRAE 51 (ANSI/AMCA 210) "*Laboratory Methods of Testing Fans for Aerodynamic Performance Rating"*, **1999**

[10] ISO 3744:1994 "*Acoustics -- Determination of sound power levels of noise sources using sound pressure -- Engineering method in an essentially free field over a reflecting plane*", International Organization for Standardization, Geneva, Switzerland, **1994**

© Jessica Gullbrand